

# Characteristics of polarization switching in vertical-cavity surface-emitting lasers

T. Ackemann, M. Sondermann

Institut für Angewandte Physik, Westfälische Wilhelms-Universität Münster,  
Corrensstraße 2/4, D-48149 Münster, Federal Republic of Germany

## ABSTRACT

Polarization selection in small-area vertical-cavity surface-emitting lasers (VCSELs) is studied experimentally in dependence on injection current and substrate temperature in the vicinity of the minimum threshold condition. Different types of polarization switching (PS) are observed and analyzed: PS from the high to the low frequency mode, PS from low to high frequency and double switching (from high to low and back to high frequency). Whereas PS from the high to the low frequency mode is due to a change of sign of linear dichroism, the optical spectra show dynamical transition states for the other case which hint to the relevance of nonlinear effects. A comparison to the predictions of the SFM-model based on phase-amplitude coupling is given. The interplay of spatial and polarization effects can depend strongly on the ambient temperature.

**Keywords:** vertical-cavity surface-emitting lasers, polarization switching, optical spectra, transverse modes, nonlinear dispersion

## 1. INTRODUCTION

Vertical-cavity surface-emitting lasers (VCSELs) have many advantageous intrinsic properties as single-longitudinal mode operation, high-speed modulation capability, easy integration with electronic circuits and – last, but not least – a circular beam profile. Therefore they are the state-of-the-art devices for short-haul fiber communication. On the other hand, their symmetric device structure is also a drawback, since it implies that the polarization state of the emitted light is only weakly pinned. Maybe the most striking manifestation of the resulting polarization instabilities is polarization switching (PS), i.e. the linear polarization state appearing at threshold is not stable but gives way to the orthogonal one as the current is increased.<sup>1-6</sup> Since any real communication system will have some polarization anisotropy, fluctuations of the polarization state will be converted to amplitude fluctuations which can degrade the performance of the system.<sup>3,5-7</sup> Polarization stability will become even more important, if VCSELs are used in future sensoric and spectroscopic applications or single-mode communication links.

Many aspects of this switching behaviour can be understood by considering linear gain or loss anisotropies for the two polarization modes which are frequency split by birefringence. The latter is due to unintentional stress left in the device after manufacturing and contacting<sup>3,8</sup> and the electro-optic effect.<sup>9</sup> If the birefringence between the two polarization modes is large enough, the low or high frequency polarization mode is favored depending on the sign of the detuning from the gain maximum.<sup>2,3</sup> Since the ohmic heating due to current flow will change the detuning, switching from the high to the low frequency mode can be induced if the current is increased. Later studies<sup>4,7</sup> confirmed that PS from the high to the low frequency mode is indeed due to a change of sign of the linear dichroism (defined as the sum of the linear gain and loss anisotropies), but that a current dependent detuning is not sufficient to explain all the observed switching scenarios.<sup>4,10,11</sup> In particular, PS was observed in pulsed operation at constant lattice temperature.<sup>12</sup> In addition, the observation of hysteresis<sup>4,13</sup> indicates that nonlinear effects might play a role in the switching.

Another approach developed by San Miguel, Feng and Moloney (SFM) relies on the spin degrees of freedom of semiconductor quantum wells.<sup>14,15</sup> Here linearly polarized emission arises from coupling of circular polarization components by the linear anisotropies. Phase-amplitude coupling as described by the  $\alpha$ -factor typical for semiconductor lasers is expected to lead to a switching from the low frequency mode to the high frequency one if the current

is increased, although the former has the higher linear (unsaturated) gain. The phenomenological introduction of the linear anisotropies and the  $\alpha$ -factor was justified recently by a microscopic model, which treats an uniaxially strained quantum well in an otherwise isotropic cavity operated at gain maximum.<sup>16,17</sup> The interplay of the linear and nonlinear mechanism is still not fully clarified: On the one hand, it appears that the steady-state polarization selection can be explained in most VCSELs without resorting to the SFM model,<sup>3,4,18</sup> on the other hand it is well established that the SFM model (or reduced versions of it) are needed to interpret the dynamical features like fluctuations and details of the optical spectra.<sup>4,7</sup> Furthermore, there are only a few studies of low to high frequency switching in VCSELs<sup>18,19</sup> and they do not report details on the optical spectra.

The situation becomes even more complicated, if spatial degrees of freedom have to be taken into account. Since the transverse extent of the active zone is typically larger than the cavity length, the Fresnel number of the cavity is larger than unity and transverse modes are excited naturally.<sup>1,20</sup> PS might appear before<sup>2,3,21,22</sup> or after<sup>3</sup> the appearance of high order transverse modes. Also a double switching from the high to the low frequency mode and back to the high one is possible, both in a single spatial mode situation<sup>23,18</sup> or if high order modes are already excited.<sup>3,21</sup> Both situations are still poorly understood. In most cases the high order mode emerging first is orthogonally polarized to the lasing fundamental one,<sup>1,3,21,22</sup> however this might be different for a strong blue detuning of the cavity resonance with respect to the gain peak.<sup>3</sup> In general the appearance of additional high order modes is strongly correlated with changes of the polarization.<sup>21</sup>

In order to clarify the characteristics of different types of PS in dependence of the detuning properties as well as the relationship between polarization and spatial states, we are going to perform a detailed experimental characterization of the properties of VCSELs in a rather broad parameter interval of current and temperature in the situation relevant for operation, i.e. around the threshold minimum and without applying additional strain. This should provide also the basis for the comparison of the experimental results with recently proposed models which combine nonlinear effects with a change of linear anisotropies due to a temperature dependence of the detuning.<sup>24,25</sup>

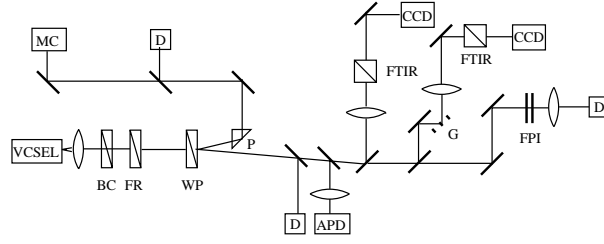
## 2. EXPERIMENTAL SETUP

Fig. 1 shows the experimental setup. The VCSEL is mounted on a temperature controlled brass-submount with a central bore which is machined to house exactly the cap of the TO46 package in order to minimize strain on the device. The emitted beam is collimated by an AR-coated aspherical lens. A Wollaston prism (WP) is used to separate the different linear polarization components. A Fresnel rhombus (FR) serves as an achromatic half-wave plate. In some experiments an additional Babinet compensator (BC) is inserted which is adjusted as a quarter-wave plate. The combination of these elements allows the projection of the light on an arbitrary polarization state, i.e. the measurement of the Stokes parameters. Large-area, low-bandwidth photodetectors (D) are used to monitor the polarization resolved light-current (LI-) characteristic of the device. Time series with a higher time resolution are obtained by an avalanche photodiode (APD, bandwidth  $> 1$  GHz, analog bandwidth of oscilloscope 750 MHz). The near field intensity distribution of the laser is imaged onto a CCD camera. The time-averaged optical spectrum is obtained by means of a plane-plane scanning Fabry-Perot interferometer (FPI) with a free spectral range of 40 GHz and a Finesse larger than 100. The system was aligned in such a way that back reflections affecting the laser were avoided. This was checked by attenuating the back reflex of the FPI by more than 43db by neutral density filters or by blocking it completely: the dynamics remains the same. A monochromator is used to measure the absolute wavelength (resolution 0.05 nm). A resolution in between the one of the monochromator and the FPI is achieved by a second spectrograph based on a holographic grating (G, 1800 lines/mm), which is used to check the result obtained with the FPI.

The devices are commercial proton-implanted samples from the company MODE (Micro Optical Devices), which operate in the 840-850 nm region. The devices are designed to work in single spatial mode (diameter of emission window 8  $\mu\text{m}$ ). Out of a bunch of seven devices, three display polarization switching in the region with a single spatial mode and four show stable operation. We will analyze the behaviour of two of these lasers, called VCSEL 1 and VCSEL 2 in the following.

## 3. EXPERIMENTAL RESULTS

Polarization resolved LI-curves were obtained by modulating the injection current of the laser by a triangular ramp with a frequency of 10 Hz at a fixed substrate temperature. For VCSEL 2 the polarization states are linear (ellipticity angle  $< 1^\circ$ ). The principal axes are aligned with the wafer axes within a few degree and do not vary by more than



**Figure 1.** Experimental setup (see text).

3 degree if the current is varied. This matches the usual observations in VCSELs.<sup>3,4</sup> From the LI-curves a stability diagram is constructed which displays the dominant polarization state in dependence on the parameters current and temperature of the active zone (Fig. 2). The latter was estimated from the substrate temperature and the current value by comparing the wavelength shift of the lasing mode (in a regime with single mode operation) with increasing current (due to ohmic heating) at constant substrate temperature with the shift occurring for increasing substrate temperature but constant current. The two fundamental spatial modes with orthogonal polarization are separated in frequency by about 10 GHz. The rhombuses denote a state in which the polarization mode with the higher frequency is on ( $P_h$ -mode), the dots a state in which the low frequency mode is on ( $P_l$ -mode). Squares denote a situation in which both modes are active. The horizontal black bars denote the value of current at which high order modes appear. Above this point, the 1:1 correspondence between polarization and frequency is lost, of course. Here, rhombuses (dots) denote that the polarization component which corresponds to the high (low) frequency fundamental mode is dominant.

The minimum threshold condition is reached for a temperature of about 44°C (corresponding to a substrate temperature of 28°C). Polarization selection is quite complicated in this device. In the low temperature region ( $\lesssim 42^\circ\text{C}$ ) the low frequency mode is selected at threshold, for high temperatures it is the high frequency mode. In addition, there is the possibility of emission on two frequencies (cf. the squares in Fig. 2), which indicates that the anisotropies which favor one of the two polarization states are very small. In that case both polarization components are excited at threshold but one of them decreases continuously again, if the current is increased slightly (see the LI-curve in Fig. 3a and the inset).

At threshold the emission is in single spatial mode but the mode quality is poor (Fig. 3b, 6.16 mA). Presumably due to an improvement of guiding due to thermal lensing, the mode quality improves if the current is increased (Fig. 3b, 8.71 mA). A dependence of the modal parameters on current is a common observation in gain-guided devices.<sup>10,26,27</sup> At about 9 mA a high order mode ( $\approx \text{TEM}_{01}$ ) appears in the weak polarization. Its power increases continuously with current. At 11.1 mA an abrupt switching takes place: The relative power of the two polarization components is reversed. At the same time the fundamental mode in the  $P_l$ -polarization switches off whereas the one in the  $P_h$ -polarization switches on. In both polarizations there are additional contributions by high order modes (Fig. 3b, 11.16 mA). If the current is increased further the relative importance of the fundamental mode in the  $P_h$ -polarization increases (Fig. 3b, 11.59 mA) and the power in the  $P_l$ -polarization nearly vanishes.

If the current is decreased again, the amplitudes of the high order modes decrease until only the fundamental mode survives in the  $P_h$ -polarization. At 7.2 mA there is a PS back to the  $P_l$ -mode. There is a huge hysteresis loop spanning from 11.1 mA till 7.2 mA.

For a threshold temperature higher than 44°C the high frequency mode emerges at threshold (Fig. 3c). If the current is increased, there is an abrupt switching (here at 5.2 mA) to the low frequency mode. If the current is ramped back and forth around the transition point hysteresis occurs (width of loop about 0.02 mA). The switching takes place in single spatial mode (Fig. 3d, 5.12 to 6.61 mA). Afterwards, the  $P_l$ -mode is active and the scenario is qualitatively the same as for lower temperatures: For increasing current the mode quality increases ( $P_l$ -mode at 9.8 mA, Fig. 3d) and a  $\text{TEM}_{01}$  appears supercritically in the weak ( $P_h$ ) polarization at about 8.6 mA. At 10.1 mA, a PS to a state dominated by a fundamental mode in the  $P_h$  direction together with some high order modes in both polarizations takes place. The width of the hysteresis loop shrinks compared to the situation for low temperature but is still considerably large (10.1 mA to 8.45 mA).

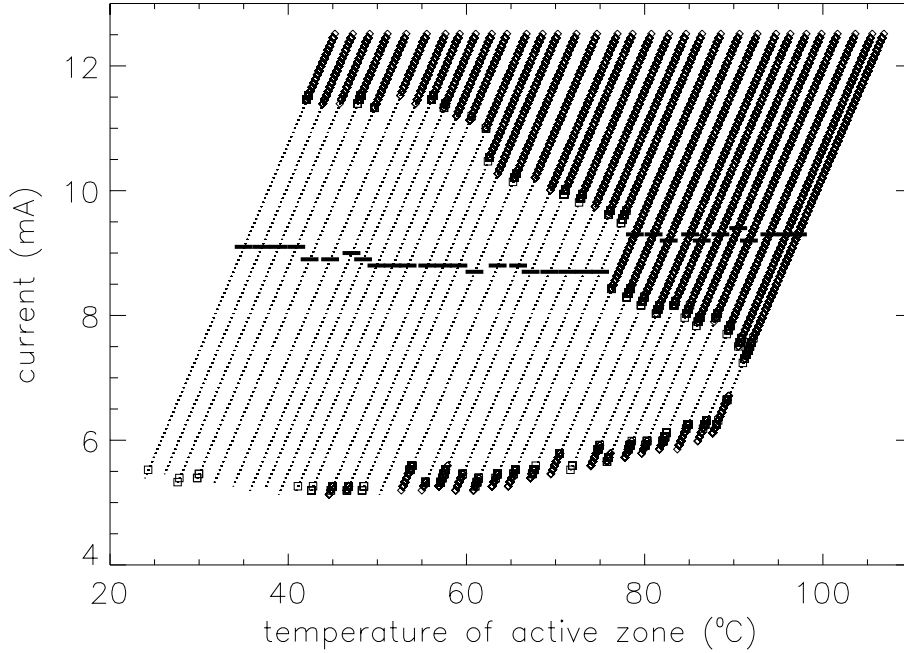


**Figure 2.** Dominant polarization state of VCSEL 2 in dependence on the parameters current and temperature of the active zone (obtained for increasing the current at constant substrate temperature). Due to ohmic heating of the active zone (3.8K/mA) the lines along which each of the measurements was done are tilted with respect to the temperature axis. The rhombuses denote a state in which the polarization mode with the higher frequency is on (or dominant), the dots a state in which the low frequency mode is on (or dominant). Squares denote a situation in which both modes are active. The horizontal black bars denote the value of current at which high order modes appear. The emission wavelength changes by 7.1 nm across the diagram.

The current value for this second switching decreases for increasing temperature until it drops below the value at which high order modes appear at a substrate temperature of 50°C (temperature of active zone about 75°C). Then a double polarization switching from the high frequency mode to the low frequency one and back to the high frequency one takes place in a purely fundamental mode situation (Fig. 3e,f).

Previous investigations<sup>4,7</sup> showed that it is fruitful to analyze the optical spectra in detail in order to extract device parameters. The common situation in VCSELs is that the spectrum is characterized by one strong lasing mode and a weak non-lasing mode, which is driven by spontaneous emission.<sup>3,4,7</sup> The frequency splitting between the polarization modes can be considered as a measure of the ‘effective birefringence’ of the cavity. We use the term ‘effective’ since it contains linear and nonlinear contributions<sup>28,4</sup> and thus depends on current. At threshold it is about 9 GHz (Fig. 4a). If the high frequency mode is lasing (i.e. before PS 1 and after PS 2) it increases with increasing current; in between it is nearly constant (Fig. 4a).

The principal form of the spectra (two Lorentzian-shaped peaks with orthogonal linear polarization) does not vary with current except in the vicinity of the second PS from the low to the high frequency mode. Here, the frequency splitting increases suddenly to about 25 GHz (Fig. 4b). The spectra are highly nonstationary and do not display well defined peaks. Observation of the dynamics close to the transition point with the avalanche photodiode reveals that the transition between the two polarization states is accompanied by stochastic hopping between two states. Histograms reveal a bimodal distribution of the intensity in an interval of 60  $\mu\text{A}$  around the transition point. This indicates the existence of bistability. Noise-induced transitions between the two coexisting states can wash out the hysteresis curve which is associated with bistability in a deterministic (or low noise) system. Bistability and noise-induced hopping between the two polarization states were analyzed for switching from the high to the low frequency mode in detail in.<sup>13</sup> Here, the interval with increased birefringence coincides with the region ( $\approx 0.06$  mA)

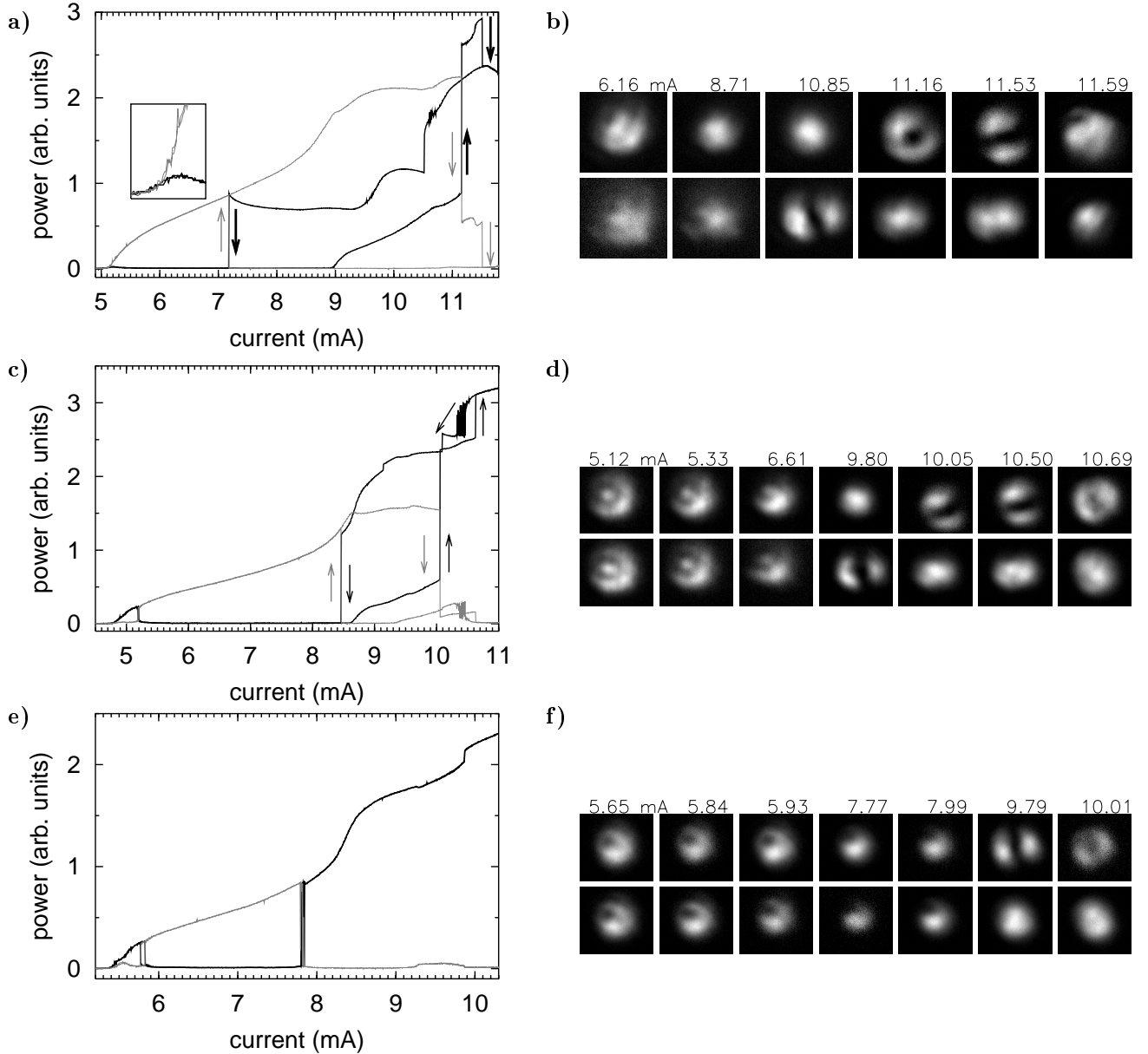


**Figure 3.** a, c, e) Polarization resolved LI-curve of VCSEL 2. Black lines represent the  $P_h$ -polarization component, grey lines the  $P_l$ -component. The inset in a) shows a magnification around threshold. b, d, f) Polarization resolved near field intensity distributions in dependence of current (upper row:  $P_l$ -polarization, lower row:  $P_h$ -polarization). The images are displayed in a linear grey level scale with white denoting high intensity. Each of the images is adjusted for maximal contrast for printing. Thus the absolute brightness carries no meaning. Substrate (threshold) temperature: a,b) 11.2°C (23°C); c,d) 33°C (48°C); e,f) 61°C (78°C).

in which bimodal intensity distributions due to stochastic hopping between two polarization states are found.

For the first PS from the high to the low frequency mode no ‘unconventional’ spectra are found. There is a hysteresis loop with a width of about 0.02 mA. By subtracting the width of the peaks in the optical spectrum one can obtain an estimation of the effective dichroism, i.e. the difference of the linear net gain (= difference between gain and loss coefficients) of the two polarization modes of the laser.<sup>4,7</sup> Fig. 5 shows that there is a minimum of

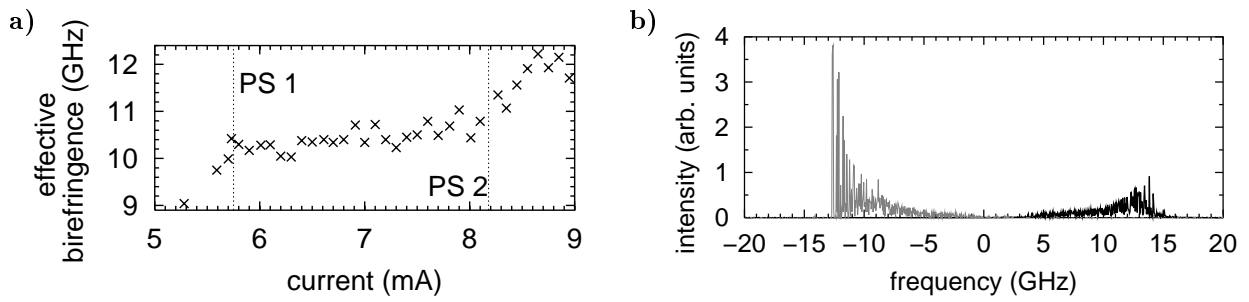


**Figure 4.** a) Effective birefringence determined from the optical spectra for VCSEL 1. b) Optical spectrum at PS 2. Substrate temperature  $56.1^\circ$ .

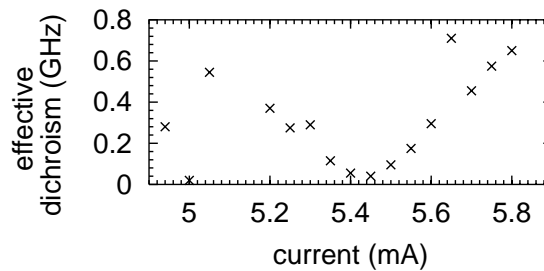


**Figure 5.** Dichroism between the two linear polarization states in the vicinity of the first PS for VCSEL 1. The values are obtained by subtracting the half width of the peaks in optical spectra averaged over 50 acquisitions. Substrate temperature  $40.6^\circ$ .

the effective dichroism at the point of the PS. Following the reasoning in<sup>4,7</sup> this observation indicates that the PS is due to a change of sign of the linear dichroism, i.e. due to a current dependence of the linear anisotropies.

In VCSEL 1 the polarization selection in dependence of parameters is simpler: The low frequency mode is selected at threshold in all the investigated range of substrate temperatures ( $10$ - $62^\circ\text{C}$ , the minimum of threshold is at about  $45^\circ\text{C}$ , Fig. 6a). PS from the low to the high frequency mode occurs for all temperatures; and the shape of the curve of the PS points has approximately the same shape as the threshold curve (Fig. 6a). The emission takes place in a fundamental spatial mode of good quality before and after the PS. High order transverse modes do not appear below a value of the injection current of  $8.5$  mA.

In contrast to the other devices we investigated, the polarization state of this laser was not linear but elliptical. Therefore it is characterized best by the complete set of Stokes parameters. From these the ellipticity angle and the direction of the major principal axis of the polarization ellipse are calculated. The result is shown in Fig. 7a. The ellipticity angle increases with increasing current from a value of  $10.5^\circ$  at threshold to  $15^\circ$  at the PS. After the PS it decreases until it is nearly zero around  $8$  mA. At threshold, the principal axis of the polarization ellipse deviates from the axis of the wafer by about  $30^\circ$  and rotates till the PS by about  $10^\circ$ . After the PS, it rotates again by about  $14^\circ$ , if the current is increased to  $8$  mA. Nevertheless, the emission is highly polarized since the fractional polarization, i.e. the sum of the normalized Stokes parameters, is greater than  $0.95$  except for a region in the vicinity of the PS (Fig. 7b).

A characterization of the optical spectra is done in another paper.<sup>29</sup> Here, we summarize briefly the results and provide further details. At threshold the birefringence is about  $5.5$  GHz and it decreases approximately linearly with current up to a certain value of current at which the character of the spectra changes. Gradually, additional peaks appear until several lasing peaks are clearly present (Fig. 6b). Each of the peaks is elliptically polarized but the main axes are different. This is in accordance with the observation that the fractional polarization drops drastically in a

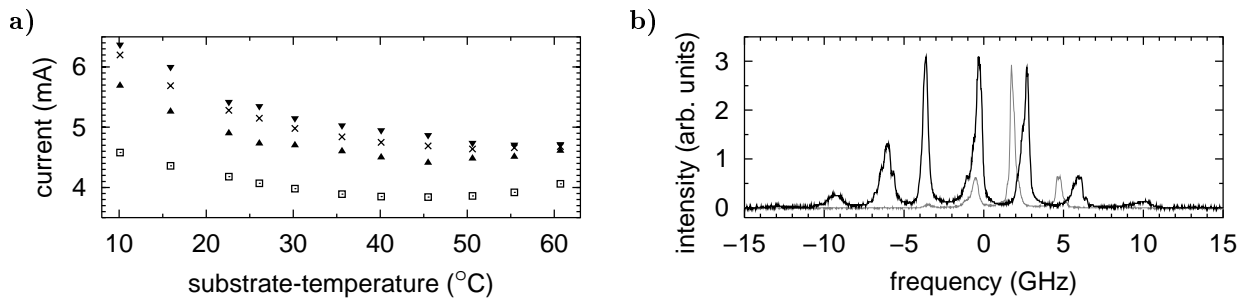


**Figure 6.** a) Laser threshold (squares), PS (crosses) and begin (up-triangles) and end (down-triangles) of current interval with dynamical states in dependence on substrate temperature for VCSEL 1. b) Optical spectra at 5.57 mA (projected on the principal axis before the PS, grey line) and at 5.7 mA (projected on the principal axis after the PS, black line). Substrate-temperature 15.9°C.

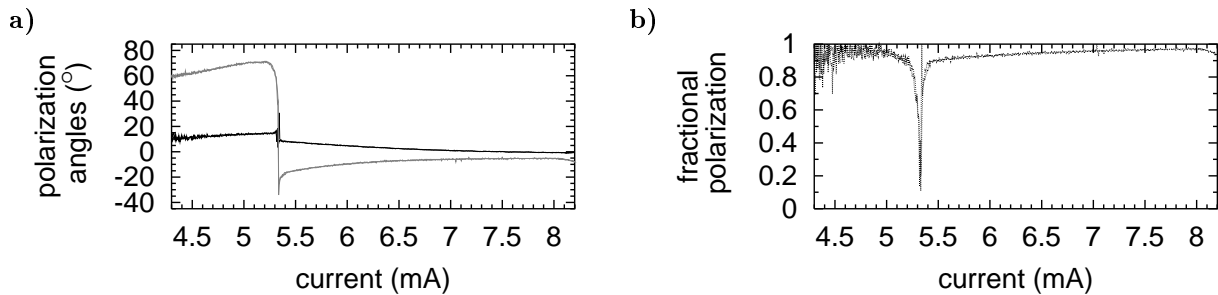


**Figure 7.** a) Direction of the major principal axis of the polarization ellipse (grey line) with respect to the wafer axis and ellipticity angle (black line). b) Fractional polarization. The vertical line denotes the PS point. The strong noise for low current is due to the fact that the signal level is small. Substrate temperature: 22.6°C.

finite region around the point of the PS (Fig. 7b). However, in contrast to the observation for VCSEL 2 (Fig. 4b) the spectrum consists still of well defined peaks. This hints to the existence of a self-pulsing of the laser on a time scale of 300 ps, which is too short to be resolved directly in the time domain by our setup.

Dynamical states appear for all temperatures (Fig. 6a). The width of the interval with dynamical states is considerably more extended than the region with a bimodal distribution and stochastic hopping between two polarization states (e.g. 0.65 mA compared to 0.03 mA for a substrate temperature of 15.9°C). However, the stochastic hopping occurs on a time scale of a few microseconds and is therefore not the origin of the appearance of multiple peaks.

For current values higher than the upper line in Fig. 6a, the spectra are ‘conventional’ again, i.e. they consist of one lasing and one non-lasing peak again. Above this line the effective birefringence increases with increasing current, i.e. there is a minimum of birefringence at the PS.

#### 4. DISCUSSION

We start with a discussion of the properties of VCSEL 1. Since the experimentally observed switching is from the low to the high frequency mode, it cannot be explained by the temperature dependent gain anisotropy proposed in.<sup>3</sup> A temperature dependence of the absorption anisotropy can cause switchings in the opposite direction<sup>18</sup> but this is considered unlikely in our case, since PS occurred for all temperatures. Furthermore, the observed spectra cannot be explained by a purely linear theory.

Hence, we will compare the experimental results to the prediction of the SFM model in the following. The original version of the SFM model<sup>15</sup> assumes isotropic gain but a loss anisotropy of the cavity. This selects one of

the two linear polarization states at threshold. The non-lasing mode of orthogonal linear polarization is separated at threshold from the lasing mode by the linear birefringence.<sup>15,28,4</sup> The non-lasing mode will red-shift with increasing current due to phase-amplitude coupling (saturable dispersion) described by the linewidth-enhancement factor.<sup>28,4</sup> If the low frequency state is selected at threshold, this implies that the effective birefringence decreases linearly with current. PS occurs if the frequency separation is zero. Afterwards the high frequency mode is lasing and the splitting increases. Thus one expects a minimum in the effective birefringence which matches our experimental observations. The change of the birefringent splitting was experimentally confirmed for the PS from a high to low frequency mode before,<sup>4</sup> but we are not aware of an investigation of the low-to-high switching counterpart.

We remark that the birefringence at threshold changes slightly in dependence of the substrate temperature. The rate is  $-0.06$  GHz/K. The origin of this effect is unclear, it might be connected to the thermal expansion of the device. Using the estimated dependence of the temperature of the active zone on current, one calculates that the birefringence might change by a rate of  $-0.16$  GHz/mA. This is far less than observed experimentally ( $-2.4$  GHz/mA before the PS in VCSEL 1) and furthermore it cannot explain the increase of the effective birefringence present in both devices if the high frequency mode is lasing. Thus we conclude that the dominant contribution to the observed change of the effective birefringence is due to saturable dispersion, whereas possible quantitative modifications due to a temperature dependence of the linear birefringence are small.

If one looks in detail, the SFM model predicts that the linear polarization state becomes unstable already slightly before the PS point and a state with stationary elliptical polarization develops.<sup>15</sup> Its main axis is slightly rotated with respect to the axis of the original linear polarization and depends also on current. If the current is increased slightly, the elliptical state becomes nonstationary. The time evolution is regular at first, but becomes chaotic for a larger current. If the current is increased slightly further, the PS occurs. Around the switching point bistability is predicted. The appearance of the nonstationary states is accompanied by a drop in the fractional polarization and the emergence of sidebands in the optical spectrum. Fig. 5 of Ref.<sup>15</sup> suggests that the polarization state of the different sidebands is elliptical but differs from peak to peak. Thus there is a rather close correspondence between the experimental observations and the theoretical predictions. The scenarios differ from each other by the fact that the amplitude of the sidebands is much higher in the experiment than in the numerical simulations. This issue certainly demands further theoretical investigations. The second difference is that the SFM model predicts elliptical states only in a small interval in the vicinity of the PS, whereas the laser in the experiment is elliptical polarized for all currents. A possible explanation is that the axes of birefringence and dichroism are not aligned.<sup>30</sup> The results in<sup>30</sup> suggest that the principal scenario for a SFM-PS does not change very much, if the misalignment is introduced. However, this point demands also further theoretical clarification. This might provide also a hint why the polarization principal axes rotate strongly in dependence of the current.

An extended version of the SFM model takes into account the frequency dependence of the gain and dispersion in a semiconductor quantum well and thus allows also for the description of temperature induced changes of the gain anisotropy.<sup>25</sup> In this model, a cavity dichroism of 0.17% is sufficient to ensure that the low frequency mode lases at threshold on both sides of the threshold minimum, even in a broader range than experimentally investigated.<sup>25</sup> This means that it is possible to reproduce the scenario observed in VCSEL 1 qualitatively in the model. Further work should be directed towards a more quantitative comparison with matching parameters in order to clarify whether the coincidence is superficial or not.

Concerning the experimental observations in VCSEL 2 we first comment on the fact that one can identify three main regions with characteristic behavior (corresponding to the subfigures of Fig. 3): For low temperatures transverse modes appear before the first PS, for medium temperatures there is first a PS and then transverse modes appear, and for high temperatures there is double switching in the fundamental mode before high order transverse modes appear. All this situations were reported separately before (cf. the introductory Section 1). However, the observation in one device – combined with a high resolution in both current and temperature – gives an indication how the various phenomena are connected to each other, whereas they appear as confusing or even conflicting observations, if the temperature (and the corresponding change of the detuning condition) is not controlled and/or monitored.

Obviously, the interplay of polarization and spatial states and the resulting switching scenarios observed in VCSEL 2 are quite complex and difficult to analyze. Whereas the curves representing the threshold for the appearance of high order modes and the second PS from low to high frequency are quite smooth everywhere, there are clear discontinuities in both curves at the point (at  $\approx 75^\circ\text{C}$  in Fig. 2) after which also the second PS occurs within the single fundamental mode regime. This indicates an interaction of the spatial and polarization degrees of freedom.



On the other hand, also on the left hand side of the discontinuity the change of the dominant polarization state does not take place by an increase of the amplitude of the orthogonally polarized high order modes, which are already present (and/or the appearance of additional high order modes) but via a switching between the fundamental modes. This hints to the possibility that basic mechanisms of polarization selection are independent of the spatial degrees of freedom and that the boundary limiting the region with dominance of the  $P_T$ -polarization state for high currents in Fig. 2 might be regarded as a single line, which is only perturbed by spatial effects. This point demands further experimental and theoretical investigations.

The observation that the PS from the high to the low frequency mode is due to a change of sign of the linear dichroism fits to the results of other groups for this type of switching.<sup>3,4</sup> Since it appears in tendency on the high frequency side of the gain maximum, it cannot be due to a shift of the detuning due to ohmic heating. A possible interpretation should start with the observation that the amplitude anisotropy is apparently quite weak at threshold since we partly observe emission in both polarization states. Also in previous investigations<sup>3</sup> a clear polarization selection was only observed if the birefringence was sufficiently high ( $> 3$  GHz in the case of Ref.<sup>3</sup>). Furthermore, anisotropies due to a difference in detuning for the two polarization modes will be smallest directly at the gain maximum. We conjecture that in this situation other mechanisms<sup>31,4,10,11</sup> also play a role in polarization selection. In our case, the strong dependence of mode quality and size on current suggests that the first PS might be related to a change of the sign of the modal gain due to thermal lensing as discussed for other gain-guided devices before.<sup>10</sup>

Double switching was observed before by other groups<sup>18</sup> but attributed to linear phenomena. However, the drastic change of the effective birefringence at the second PS point indicates the importance of nonlinear phenomena in our device. The increase of the effective birefringence in dependence on current observed in VCSEL 1 (Fig. 4a) if the high frequency mode is active is in accordance with the expectation from the SFM model.<sup>28,4</sup> It is unclear, why the birefringence remains approximately constant if the low frequency mode is lasing (Fig. 4a). In the extended SFM model<sup>25</sup> double switching is possible, in principle, and dynamical states exist before the second PS,<sup>32</sup> but more analysis needs to be done, before a connection between this theoretical prediction and the experimental results can be claimed.

## 5. CONCLUDING REMARKS

In summary, PS in VCSELs was studied experimentally with an emphasis on the case of switching from the low to the high frequency mode. The observation of dynamical transition states hints to the relevance of nonlinear effects. Similar effects are predicted by the SFM model based on nonlinear dispersion. For an understanding of the interplay of spatial and polarization degrees of freedom it is essential to analyze the behavior in a rather wide interval of temperature, respectively detuning.

The investigations are complicated by the fact that there are large deviations in behavior from device to device since anisotropies in electrically pumped VCSELs are difficult to control. Therefore it is necessary to study as many devices and types of devices as possible. Our work is meant to fit in this framework. The results indicate that – at least in some VCSELs – nonlinear effects are not only important for the dynamical characteristics of VCSELs but also for the selection of the stationary polarization states.

## ACKNOWLEDGMENTS

We thank M. San Miguel, S. Balle, C. Mirasso and J. Mulet for fruitful discussions on the SFM model and W. Lange for providing the possibility to perform the experiments in his lab.

## REFERENCES

1. C. J. Chang-Hasnain, J. P. Harbison, G. Hasnain, A. Von Lehmen, L. T. Florez, and N. G. Stoffel, “Dynamic, polarization and transverse mode characteristics of vertical cavity surface-emitting lasers,” *IEEE J. Quantum Electron.* **27**, pp. 1402–1409, 1991.
2. K. D. Choquette, D. A. Richie, and R. E. Leibenguth, “Temperature dependence of gain-guided vertical-cavity surface emitting laser polarization,” *Appl. Phys. Lett.* **64**, pp. 2062–2064, 1994.
3. K. D. Choquette, R. P. Schneider Jr., K. L. Lear, and R. E. Leibenguth, “Gain dependent polarization properties of vertical cavity surface-emitting lasers,” *IEEE J. Sel. Top. Quantum Electron.* **1**, pp. 661–666, 1995.

4. M. P. v. Exter, M. B. Willemsen, and J. P. Woerdman, "Polarization fluctuations in vertical-cavity semiconductor lasers," *Phys. Rev. A* **58**, pp. 4191–4205, 1998.
5. D. V. Kuksenkov, H. Temkin, and S. Swirhun, "Polarization instability and relative intensity noise in vertical-cavity surface-emitting lasers," *Appl. Phys. Lett.* **67**, pp. 2141–2143, 1995.
6. D. V. Kuksenkov, H. Temkin, and S. Swirhun, "Polarization instability and performance of free-space optical links based on vertical-cavity surface-emitting laser," *IEEE Photon. Technol. Lett.* **8**, pp. 703–705, 1996.
7. M. P. v. Exter, M. B. Willemsen, and J. P. Woerdman, "Polarization modal noise and dichroism in vertical-cavity semiconductor lasers," *Appl. Phys. Lett.* **74**, pp. 2274–2276, 1999.
8. A. K. v. Doorn, M. P. v. Exter, and J. P. Woerdman, "Elasto-optic anisotropy and polarization orientation of vertical-cavity surface-emitting semiconductor lasers," *Appl. Phys. Lett.* **69**, pp. 1041–1043, 1996.
9. R. F. M. Hendriks, M. P. v. Exter, J. P. Woerdman, A. van Geelen, L. Weegels, K. H. Gulden, and M. Moser, "Electro-optic birefringence in semiconductor vertical-cavity lasers," *Appl. Phys. Lett.* **71**, pp. 2599–2601, 1997.
10. K. Panajotov, B. Ryvkin, J. Danckaert, M. Peeters, H. Thienpont, and I. Veretennicoff, "Polarization switching in VCSEL's due to thermal lensing," *IEEE Photon. Technol. Lett.* **10**, pp. 6–8, 1998.
11. B. S. Ryvkin and A. Georgievskii, "Polarization selection in VCSELs due to current carrier heating," *Semiconductors* **33**(7), pp. 813–819, 1999.
12. J. Martín-Regalado, J. L. A. Chilla, J. J. Rocca, and P. Brusenbach, "Polarization switching in vertical-cavity surface-emitting lasers observed at constant active region temperature," *Appl. Phys. Lett.* **70**, pp. 3350–3352, 1997.
13. M. B. Willemsen, M. U. F. Khalid, M. P. van Exter, and J. P. Woerdman, "Polarization switching of a vertical-cavity semiconductor laser as a Kramers hopping problem," *Phys. Rev. Lett.* **82**, pp. 4815–4813, 1999.
14. M. San Miguel, Q. Feng, and J. V. Moloney, "Light polarization dynamics in surface-emitting semiconductor lasers," *Phys. Rev. A* **52**, pp. 1728–1739, 1995.
15. J. Martín-Regalado, F. Prati, M. San Miguel, and N. B. Abraham, "Polarization properties of vertical-cavity surface-emitting lasers," *IEEE J. Quantum Electron.* **33**, pp. 765–783, 1997.
16. D. Burak, J. V. Moloney, and R. Binder, "Microscopic theory of polarization properties of optically anisotropic vertical-cavity surface-emitting lasers," *Phys. Rev. A* **61**, p. 053809, 2000.
17. D. Burak, J. V. Moloney, and R. Binder, "Microscopic versus macroscopic description of polarization properties of optically anisotropic vertical-cavity surface-emitting lasers," *IEEE J. Quantum Electron.* **36**, pp. 956–970, 2000.
18. B. Ryvkin, K. Panajotov, A. Georgievski, J. Danckaert, M. Peeters, G. Verschaffelt, H. Thienpont, and I. Veretennicoff, "Effect of photon-energy-dependent loss and gain mechanisms on polarization switching in vertical-cavity surface-emitting lasers," *J. Opt. Soc. Am. B* **16**, pp. 2106–2113, 1999.
19. M. B. Willemsen, M. P. v. Exter, and J. P. Woerdman, "Anatomy of a polarization switch of a vertical-cavity semiconductor laser," *Phys. Rev. Lett.* **84**, pp. 4337–4340, 2000.
20. H. Li, T. L. Lucas, J. G. McInerney, and R. A. Morgan, "Transverse modes and patterns of electrically pumped vertical-cavity surface-emitting semiconductor diodes," *Chaos, Solitons & Fractals* **4**, pp. 1619–1636, 1994.
21. J. E. Epler, S. Gehrsitz, K. H. Gulden, M. Moser, H. C. Sigg, and H. E. Lehmann, "Mode behavior and high resolution spectra of circularly-symmetric GaAs-AlGaAs air-post vertical cavity surface emitting lasers," *Appl. Phys. Lett.* **69**, pp. 722–724, 1996.
22. U. Fiedler, G. Reiner, P. Schnitzer, and K. J. Ebeling, "Top vertical-cavity surface-emitting laser diodes for 10-Gb/s data transmission," *IEEE Photon. Technol. Lett.* **8**, pp. 746–748, 1996.
23. K. D. Choquette, K. L. Lear, R. E. Leibenguth, and M. T. Ascom, "Polarization modulation of cruciform vertical-cavity laser diodes," *Appl. Phys. Lett.* **64**, pp. 2767–2769, 1994.
24. S. Balle, E. Tolkacheva, M. San Miguel, J. R. Tredicce, J. Martín-Regalado, and A. Gahl, "Mechanisms of polarization switching in single-transverse-mode VCSELs: Thermal shift and nonlinear semiconductor dynamics," *Opt. Lett.* **24**, pp. 1121–1123, 1999.
25. M. San Miguel, S. Balle, J. Mulet, C. Mirasso, E. Tolkachova, and J. R. Tredicce, "Combined effects of semiconductor gain dynamics, spin dynamics and thermal shift in polarization selection in VCSELs," *Proc. SPIE.* **3944**, pp. 242–251, 2000.
26. D. Vakhshoori, J. D. Wynn, G. J. Zydzik, R. E. Leibenguth, M. T. Asom, K. Kojima, and R. A. Morgan, "Top-surface emitting lasers with 1.9 V threshold voltage and the effect of spatial hole burning on their transverse mode operation and efficiencies," *Appl. Phys. Lett.* **62**, pp. 1448–1450, 1993.

27. X. Tang, J. P. van der Ziel, B. Chang, R. Johnson, and J. A. Tatum, "Observation of bistability in GaAs quantum-well vertical-cavity surface-emitting lasers," *IEEE J. Quantum Electron.* **33**, pp. 927–932, 1997.
28. H. Lem and D. Lenstra, "Saturation-induced frequency shift in the noise spectrum of a birefringent vertical-cavity surface-emitting laser," *Opt. Lett.* **22**, pp. 1698–1700, 1997.
29. T. Ackemann and M. Sondermann, "Characteristics of polarization switching from the low to the high frequency mode in vertical-cavity surface-emitting lasers,". Submitted to *Appl. Phys. Lett.*, 2000.
30. M. Travagnin, "Linear anisotropies and polarization properties of vertical-cavity surface-emitting semiconductor lasers," *Phys. Rev. A* **56**, pp. 4094–4105, 1997.
31. A. Valle, K. A. Shore, and L. Pesquera, "Polarization selection in birefringent vertical-cavity surface emitting lasers," *Journal of Lightwave Technology* **14**(9), pp. 2062–8, 1996.
32. J. Mulet, S. Balle, C. R. Mirasso, and M. San Miguel, "Transverse and polarization mode selection in vertical-cavity surface-emitting lasers," in *European workshop on VCSELs: from physics to applications*, Brussels, August, 28-30, 2000. Paper P1.